RSC Advances

ROYAL SOCIETY OF CHEMISTRY

www.rsc.org/advances

Cite this: DOI: 10.1039/c0xx00000x

www.rsc.org/xxxxxx

ARTICLE TYPE

Striking influence of NiO catalyst diameter on the carbonization of polypropylene into carbon nanomaterials and their high performance in the adsorption of oils†

Jiang Gong[a,b], Jie Liu*[a], Xuecheng Chen[a,c], Zhiwei Jiang[a,b], Xin Wen[a], Ewa Mijowska[c], Tao Tang*[a]

Received (in XXX, XXX) Xth XXXXXXXXX 200X, Accepted Xth XXXXXXXXX 200X
DOI: 10.1039/b000000x

Recently, there has been intense interest in the conversion of plastics into high value-added carbon nanomaterials (CNMs), however, the effect of catalyst diameter on the formation of CNMs is still ambiguous. Herein, uniform NiO catalysts with different diameter (18–227 nm) were firstly prepared by sol-gel combustion synthesis method and calcination at different temperature. Subsequently, the combined organically-modified montmorillonite (OMMT)/NiO catalyst was used to catalyze carbonization of polypropylene (PP, selected as an example of plastics) into CNMs at 700 °C. The effect of NiO catalyst diameter on the yield, morphology, microstructure, phase structure, thermal stability and texture property of CNMs including sponge-like cup-stacked carbon nanotubes (CS-CNTs) and carbon fibers were investigated by scanning electron microscope, transmission electron microscope (TEM), high-resolution TEM, X-ray diffraction, Raman spectroscopy, thermal gravimetric analysis and N_2 sorption. Besides, the effects of NiO catalyst diameter on the coalescence and reconstruction of NiO particles were explored. It was demonstrated that NiO catalysts with small diameter were more susceptible to the coalescence and reconstruction into rhombic shape, which facilitated the growth of long, straight CS-CNTs. Finally, the obtained sponge-like CS-CNTs were found to show high performance in the adsorptions of diesel, vegetable oil, kerosene and mineral oil with good recycling performance. It is believed that this work will contribute to the conversion of waste plastics into high value-added CNMs.

1. Introduction

Recently, the growth of high value-added carbon nanomaterials (CNMs) such as carbon nanotubes (CNTs) using plastics as carbon sources has become an emerging method.[1,2] This is because the total amount of waste plastics generated by human society is increasing (*e.g.*, from 1.7 million tons in 1950 to 280 million tons in 2011),[1] and becoming a serious environmental problem. The tradition disposal ways of waste plastics are landfill and incineration, but they waste resources and harm the environment. So far, much progress has been made on converting plastics including polypropylene (PP), polyethylene (PE) and polystyrene (PS) into CNMs with diverse morphologies such as CNTs, cup-stacked CNTs (CS-CNTs), carbon nanofibers (CNFs) and carbon spheres (CSs). For example, Wu *et al.* used catalytic gasification to process PP and PS into CNTs with hydrogen-rich synthetic gas by Ni/Ca–Al or Ni/Zn–Al catalyst.[3,4] Acomb *et al.* used pyrolysis-gasification of PP, PE and PS to prepare CNTs by Ni/Al_2O_3 catalyst.[5] Zhuo *et al.* reported the synthesis of CNTs and CNFs from PE using stainless-steel wire mesh as catalyst by a novel pyrolysis–combustion technique.[6,7] Pol *et al.* used autoclave as reactor to convert PE into CNTs using $Co(Ac)_2$ as catalyst under high pressure.[8] Our group put forward a strategy of combined degradation catalyst/carbonization catalyst, including solid acids (such as OMMT or zeolite)/nickel catalyst,[9−13] halogenated compounds/Ni_2O_3 (ref. 14−17), and activated carbon/Ni_2O_3,[18] to convert PP, PE and PS into CNTs, CS-CNTs, CNFs and CSs[19, 20] under atmospheric condition.

Unfortunately, the quality of CNTs from plastics is yet needed to be improved. As well known to all, the catalyst diameter is one of the key factors that affect the growth of CNTs, but still controversial. For example, there were several reports, which supported such an idea that the diameter of CNTs was strongly influenced by the catalyst diameter,[21,22] whereas others claimed that there was no correlation between the diameter of catalyst nanoparticles and that of synthesized CNTs.[23,24] Until now, there are no reports focusing on the effect of catalyst diameter on the carbonization of plastics into CNMs. Recently, we found that the coalescence and reconstruction of NiO nanoparticles into rhombic shape during the carbonization of PP were crucial for the growth of long, straight and smooth-surface CS-CNTs.[12,17] Hence, how does the diameter of NiO catalyst influence the yield, morphology and microstructure of CS-CNTs? How does the diameter of NiO catalyst affect the coalescence and reconstruction of NiO nanoparticles? Solving these questions is particularly important to further understand the carbonization mechanism of plastics and convert waste plastics into high value-added CNMs.

Furthermore, although many investigations have been conducted to transform plastics into CNMs with diverse morphologies,[3–20] to the best of our knowledge, there are no reports about synthesizing sponge-like CNTs using plastics as carbon sources. Sponge-like CNTs have the characteristics such as light weight, high porosity and large surface area, which make them promising candidates for environmental application such as sorption, filtration and separation.[25,26] Gui *et al.* used 1,2-dichlorobenzene as carbon source *via* chemical vapor deposition to prepare sponge-like CNTs, which showed excellent performance in the adsorption of oils with good mechanical flexibility.[27] However, much reaction time (4 hours) was needed to prepare sponge-like CNTs. Thereby, it is of great desire to explore a simple way to efficiently convert plastics into sponge-like CNTs.

Herein, a one-pot approach was established to efficiently synthesize sponge-like CS-CNTs through the carbonization of PP (selected as an example of plastics) using the combined catalysts of OMMT and NiO at 700 °C. The effect of NiO catalyst diameter on the yield, morphology, microstructure, phase structure, thermal stability and texture property of sponge-like CS-CNTs were fully investigated. In addition, the effects of NiO catalyst diameter on the coalescence and reconstruction of NiO particles were explored. Finally, the obtained sponge-like CS-CNTs were used as adsorbents for diesel, vegetable oil, kerosene and mineral oil. It is believed that this work will contribute to the conversion of waste plastics into high value-added CNMs.

2. Experiment part

2.1 Materials

Polypropylene (PP, weight-average molecular weight = 3.07 × 10^5 g/mol, polydispersity index = 3.13, and trademark T30S) powder was supplied by Yanan Petrochemical Co., China. OMMT (Closite 15A, organic modifier: dimethyl-dihydrogenated tallow quarternary ammonium, and modifier concentration: 125 mequiv per 100 g clay) was purchased from Southern Clay. NiO catalysts with different diameter were prepared by sol-gel combustion synthesis method, followed by calcination at different temperature. Firstly, precursor solution was prepared as following: 29.08 g $Ni(NO_3)_2{\cdot}6H_2O$ (analytical reagent, supplied from Beijing Chemical Works) and 5.76 g citric acid (analytical reagent, provided by Beijing Chemical Works) were dissolved in 200 mL deionized water. The solution was then evaporated at 80 °C until forming gel, which was further heated under air at the temperature of self-ignition. After ignition, the obtained NiO was calcined at different temperature (400–900 °C) for 2 hours in a muffle oven and designated as NiO-x, where x represented the calcination temperature. The resultant NiO-x catalyst was used as carbonization catalyst to synthesize CNMs.

2.2 Preparation of samples

PP powder (40.00 g) was mixed with NiO-x (3.00 g) and OMMT (0.50 g) in a Brabender mixer at 100 rpm and 180 °C for 10 min. The resultant sample was designated as PP/OMMT-NiO-x. For comparison, PP/NiO-x with NiO-x content of 7.5 (g/100 g PP) and PP/OMMT with OMMT content of 1.25 (g/100 g PP) were also prepared.

2.3 Preparation of CNMs

CNMs were prepared through carbonization experiment by heating PP/OMMT-NiO-x in a crucible at 700 °C according to our previous report.[14] Briefly, a piece of PP/OMMT-NiO-x (5.2–5.5 g) was placed into a crucible, which was heated at 700 °C for 5 min. The resultant CNMs were cooled to room temperature, weighed and designated as CNM-y, where y represented the average diameter of NiO-x in the PP/OMMT-NiO-x. The yield of CNM-y was calculated by dividing the amount of the obtained carbon (the amount of the residue after subtracting the amount of the residual catalysts) by that of carbon element in the PP from PP/OMMT-NiO-x. Each measurement was repeated four times for reproducibility purpose.

2.4 Characterization

The morphologies of NiO-x and CNMs were observed by field-emission scanning electron microscope (FE-SEM, XL30ESEM-FEG) and transmission electron microscope (TEM, JEM-1011) at an accelerating voltage of 100 kV. The microstructure of CNMs was investigated using high-resolution TEM (HRTEM) performed on a FEI Tecnai G2 S-Twin transmission electron microscope operating at 200 kV. The phase structures of NiO-x and CNMs were analyzed by X-ray diffraction (XRD) using a D8 advance X-ray diffractometer with Cu Kα radiation operating at 40 kV and 200 mA. The vibrational property of CNMs was characterized by Raman spectroscopy (T6400, excitation-beam wavelength: 514.5 nm). The thermal stability of CNMs was measured by thermal gravimetric analysis (TGA) under air flow at a heating rate of 10 °C/min using a TA Instruments SDT Q600. The textural property of CNMs was measured by N_2 sorption at 77 K using a Quantachrome Autosorb-1C-MS analyzer. The specific surface area was calculated by BET method, and the contribution of micropores to both volume and surface area was evaluated by the *t*-plot method.

2.5 Adsorption experiments

According to the method reported previously,[27,28] the adsorption experiments of oils including diesel, vegetable oil, kerosene and mineral oil by the resultant CNMs were carried out in a glass beaker (150 mL) covered with a piece of metal sieve. An amount of 0.1 g CNMs was put into the beaker first and then 50 mL of oil was poured into the beaker. After 5 min, the beaker was placed upside down and left still to drain off the excess oil. The adsorption was fast and typically reached the equilibrium stage in a few minutes. The CNMs were then collected by the metal sieve and weighed. The oil adsorption capacity (g/g) of CNMs was calculated as $(W-W_0)/W_0$, where W is the weight of CNMs after oil adsorption and W_0 is the weight of CNMs before oil adsorption. To study the reusability of CNMs, the recovered CNM-40 was calcined at in a muffle at 400 °C for 1 hour and reused as adsorbent for six cycles.

3. Results and discussion

3.1 Characterization of NiO catalysts

The XRD patterns of NiO catalysts calcined at different temperature are shown in Fig. 1. Characteristic diffraction peaks of face-centered cubic NiO at 2θ = 37.6° (111), 43.6° (200), 63.2°

(220), 75.7° (311) and 79.7° (222) were observed in the resultant NiO catalysts, and no diffraction peaks of metallic nickel were detected. Besides, it was noticeable that all the characteristic peaks of NiO became narrow and sharpened with increasing calcination temperature, which indicated the increase in the degree of crystallinity of NiO catalysts. This was because the annealing treatment conducted at high temperature healed the defect of crystals, giving the NiO catalyst of better crystallinity.

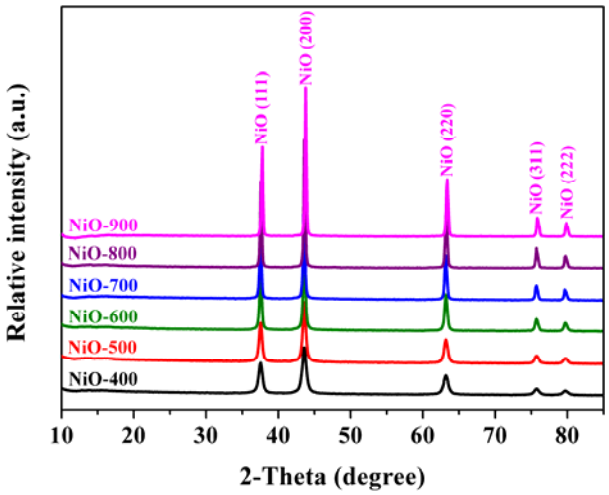

Fig. 1 XRD patterns of NiO catalysts calcined at different temperature.

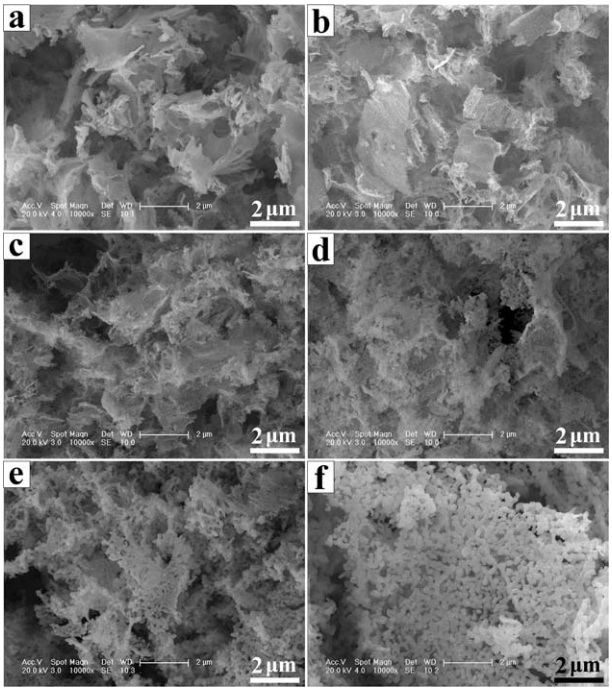

Fig. 2 Typical FE-SEM images of NiO catalysts calcined at different temperature: (a) NiO-400, (b) NiO-500, (c) NiO-600, (d) NiO-700, (e) NiO-800 and (f) NiO-900.

Fig. 2 shows the typical FE-SEM images of NiO catalysts calcined at different temperature. Obviously, the resultant NiO catalysts were lamellar structure ranging from hundreds of nanometers to several micrometers in length. When the calcination temperature increased up to 700 °C, the lamella of NiO became porous and many particles were observed clearly. TEM images of NiO catalysts (Fig. 3) further demonstrated that all of NiO catalysts consisted of uniform particles. The size distribution histograms of NiO particles are shown in Fig. S1 in ESI†. The average diameter of NiO particles was 18 ± 3 nm for NiO-400, 26 ± 5 nm for NiO-500, 40 ± 11 nm for NiO-600, 96 ± 18 nm for NiO-700, 128 ± 25 nm for NiO-800, and 227 ± 40 nm for NiO-900.

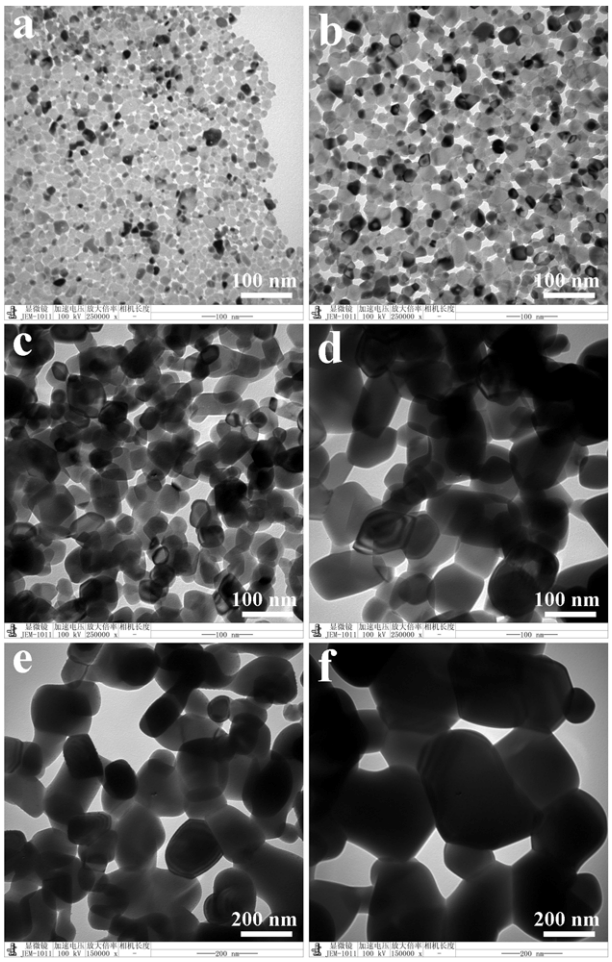

Fig. 3 Typical TEM images of NiO catalysts: (a) NiO-400, (b) NiO-500, (c) NiO-600, (d) NiO-700, (e) NiO-800 and (f) NiO-900.

3.2 Effect of NiO catalyst diameter on the yield of CNMs

Fig. 4 shows the effect of NiO catalyst diameter on the yield of CNMs from PP/OMMT-NiO-x at 700 °C. In the case of PP/NiO-x or PP/OMMT, the yield of CNMs was less than 7.0 or 1.0 wt %, respectively, indicating that NiO-x with different diameter or OMMT alone could not effectively catalyze carbonization of PP. However, after adding OMMT (1.25 g/100 g PP) into PP/NiO-x, the yield of CNMs increased. For example, the yield of CNMs increased from 6.8 wt % for PP/NiO-400 to 51.9 wt % for PP/OMMT-NiO-400. However, when the diameter of NiO catalyst increased from 18 nm (NiO-400) to 227 nm (NiO-900),

the yield of CNMs almost linearly decreased from 51.9 wt % for PP/OMMT-NiO-400 to 10.8 wt % for PP/OMMT-NiO-900. This result demonstrated that the combined OMMT/NiO-400 showed much higher catalytic efficiency than OMMT/NiO-900 in the carbonization of PP into CNMs. Thus the catalytic ability of NiO-400 was much higher than that of NiO-900, since the carbon source (*i.e.*, the degradation products of PP under the catalysis of OMMT) was actually the same. Consequently, the diameter of NiO catalyst played an important role in the catalytic carbonization of PP into CNMs.

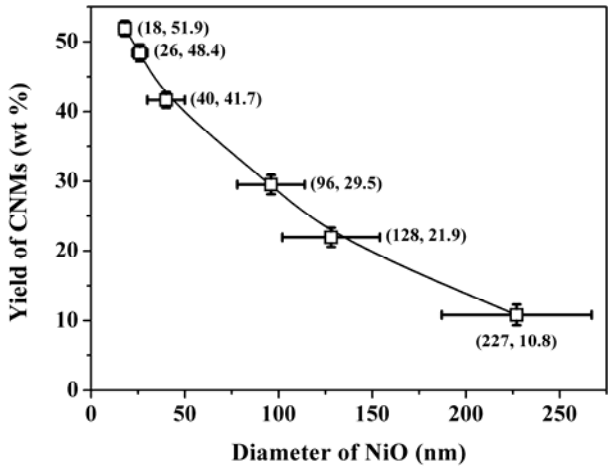

Fig. 4 Effect of NiO catalyst diameter on the yield of CNMs from PP/OMMT-NiO-x at 700 °C.

3.3 Effects of NiO catalyst diameter on the macrostructure, morphology and microstructure of CNMs

Fig. 5 presents the photographs of PP/OMMT-NiO-x and the resultant CNMs. It was observed that after the carbonization of PP/OMMT-NiO-x (Fig. 5a), soft carbon was obtained in the CNM-18, CNM-26, CNM-40 and CNM-96, while CNM-128 and CNM-227 were loose hard powder (Fig. 5b). Especially, CNM-40 could be removed out of the crucible without damaging the crucible-like shape of CNM-40, and showed to be sponge-like carbon with high strength and flexibility (Fig. 5c).

Fig. 5 Photographs of (a) PP/OMMT-NiO-x (5.2−5.5 g) in the crucible (30 mL), (b) CNMs from PP/OMMT-NiO-x after being removed off the crucible, and (c) the crucible (25.6 g) supported by sponge-like CNM-40 (2.2 g). Crucible 1# was marked for PP/OMMT-NiO-400 or CNM-18, crucible 2# for PP/OMMT-NiO-500 or CNM-26, crucible 3# for PP/OMMT-NiO-600 or CNM-40, crucible 4# for PP/OMMT-NiO-700 or CNM-96, crucible 5# for PP/OMMT-NiO-800 or CNM-128, and crucible 6# for PP/OMMT-NiO-900 or CNM-227.

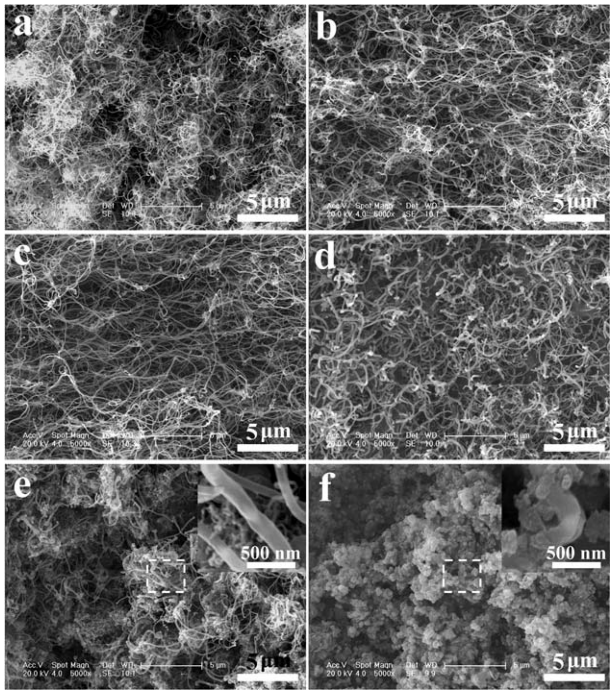

Fig. 6 Typical FE-SEM images of CNMs from PP/OMMT-NiO-x: (a) CNM-18, (b) CNM-26, (c) CNM-40, (d) CNM-96, (e) CNM-128 and (f) CNM-227. The inset images showed the higher magnification of the marked regions by white dashed line.

To investigate whether the diameter of NiO catalyst had any effects on the morphology and microstructure of CNMs, FE-SEM, TEM and HRTEM observations were performed on the resultant CNM-x from PP/OMMT-NiO-x. Fig. 6 shows the typical FE-SEM images of the resultant CNMs. Strikingly, when the diameter of NiO catalyst was 18 or 26 nm, a lot of relative long, straight and small filamentous carbon were obtained in the CNM-18 and CNM-26 (Figs. 6a and 6b). When the diameter of NiO catalyst increased to 40 nm, filamentous carbon in the resultant CNM-40 became longer, and the diameter showed no obvious changes (Fig. 6c). However, filamentous carbon became shorter when the diameter of NiO catalyst increased to 96 nm (Fig. 6d). Interestingly, when the diameter of NiO catalyst further increased to 128 or 227 nm, there were a great amount of relatively larger and shorter filamentous carbon in the obtained CNM-128 or CNM-227 (Figs. 6e and 6f).

Fig. 7 displays the typical TEM images of the corresponding CNMs. The resultant relatively straight and long filamentous carbon from CNM-18, CNM-26, CNM-40 and CNM-96 had a typical tubular-like form (Figs. 7a–7d), which is characteristic of CNTs. Further HRTEM observation demonstrated that the graphitic layers in the long and straight CNTs from CNM-40 were oblique to the CNT axis at the angle of 20–23° (Fig. 8). On the basis of this result, the obtained CNTs are identified as CS-CNTs,[29] which are different from conventional CNTs made up of multi-seamless cylinders of hexagonal carbon networks. As a result, a large portion of exposed and reactive edges with abundant dangling bonds exist on the outer surface and in the inner channel of CS-CNTs,[30] which makes them excellent candidates in the applications of nanoelectronics,[31] absorbents,[17,32] nancomposites,[33] energy,[34] electrochemical biosensors,[35] and heterogeneous catalysis,[36] *etc*. The surface of

CS-CNTs seemed to be smooth and they had narrow diameter and length distributions (Figs. S2 and S3). The mean outer diameter and length were 46 nm and 7.2 μm for CNM-18, 49 nm and 9.6 μm for CNM-26, 57 nm and 17.9 μm for CNM-40, and 72 nm and 5.1 μm for CNM-96 (Fig. 9). Comparatively, larger and shorter CFs with a wide diameter distribution were found in both CNM-128 and CNM-227, and the surface of CFs was rough (Figs. S2 and S3). The mean outer diameter and length of CNM-128 and CNM7.5-227 were 126 nm and 2.5 μm, and 247 nm and 0.5 μm, respectively (Fig. 9). Interestingly, the shape of CFs from CNM-227 seemed to be alphabet letter "V", and thus they were named as V-type CFs to distinguish from CNM-128. According to the above results, a conclusion could be drawn that the diameter of NiO catalyst remarkably affected the macrostructure, morphology and microstructure of CNMs from the carbonization of PP.

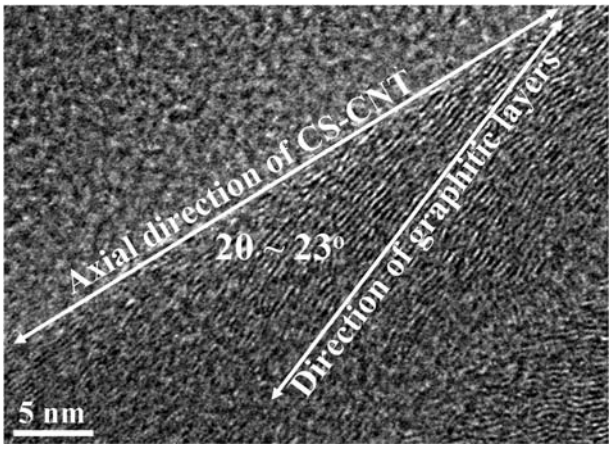

Fig. 8 HRTEM image of CNM-40.

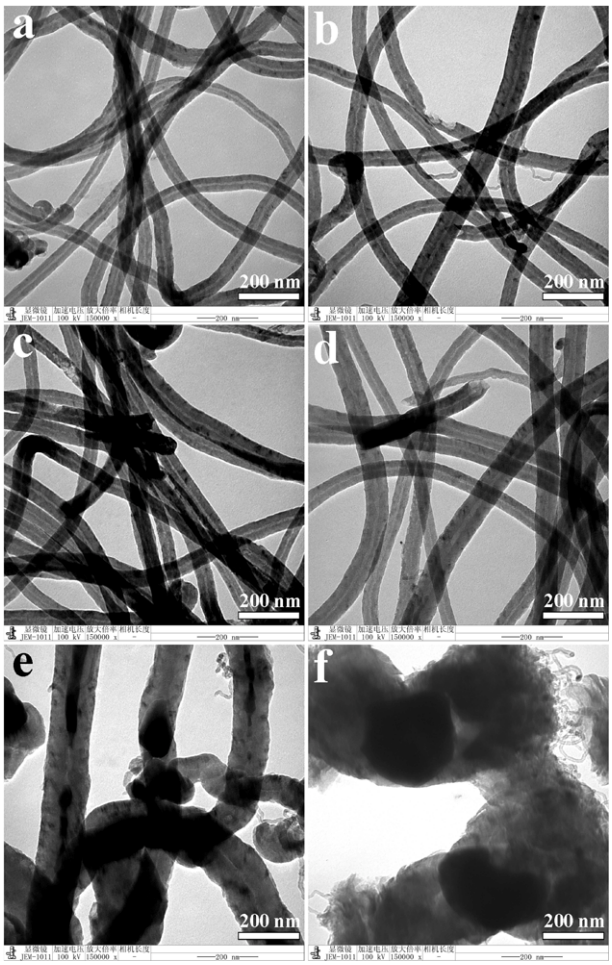

Fig. 7 Typical TEM images of CNMs from PP/OMMT-NiO-x: (a) CNM-18, (b) CNM-26, (c) CNM-40, (d) CNM-96, (e) CNM-128 and (f) CNM-227.

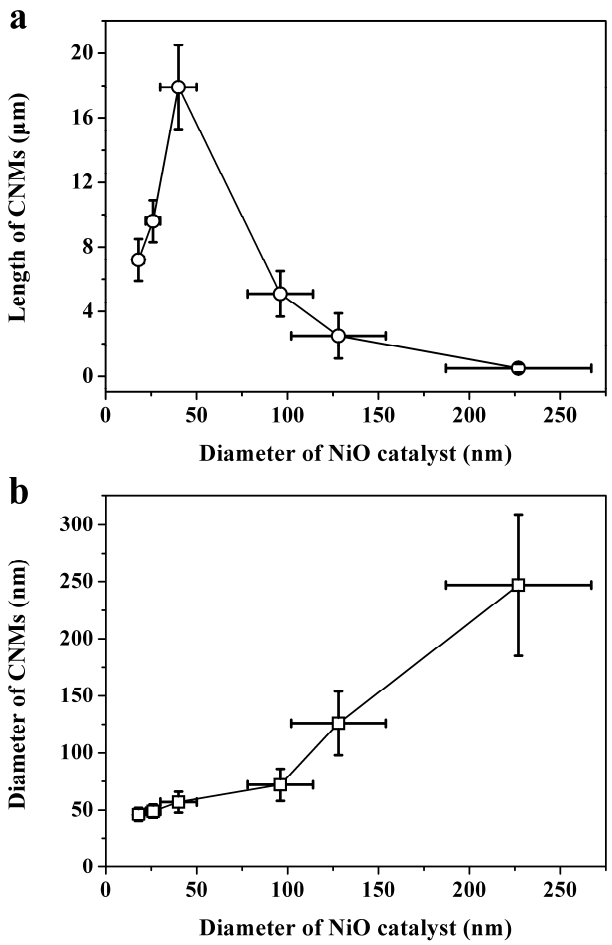

Fig. 9 Effects of the diameter of NiO catalyst on the length (a) and diameter (b) of CNMs from PP/OMMT-NiO-x.

3.4 Effects of NiO catalyst diameter on the phase structure and thermal stability of CNMs

XRD, Raman and TGA measurements were conducted to further study the effects of NiO catalyst diameter on the phase structure and thermal stability of CNMs. Fig. 10 displays the XRD patterns of the resultant CNMs. Characteristic diffraction peaks of both

graphite (2θ = 26.5° (002) and 43.4° (101)) and metallic Ni (2θ = 44.8° (111), 52.3° (200) and 76.8° (220)) were observed. This indicated that NiO was reduced into metallic nickel during the carbonization of PP, which was the real active site for the growth of CS-CNTs or CFs. Furthermore, the intensity ratio of diffraction peak of graphite (002) to that of metallic nickel (111) in the CNM-18, CNM-26, CNM-40 or CNM-96 was obviously larger than that from CNM-128 or CNM-227. This suggested that CS-CNTs contained less lattice distortions than CFs. Characteristic diffraction peak of MMT from the decomposition of OMMT was also observed at 2θ = 14.5°. Fig. 11 presents the Raman spectra of the corresponding CNMs. The peak at about 1580 cm^{-1} (*G* band) corresponds to an E_{2g} mode of hexagonal graphite and is related to the vibration of sp^2-bonded carbon atoms in a graphite layer, and the *D* band at about 1345 cm^{-1} is associated with vibration of carbon atoms with dangling bonds in the plane terminations of disordered graphite or glassy carbons. A larger I_G/I_D ratio indicates a higher degree of structural ordering for CNMs.[37–39] The I_G/I_D ratio was 0.57 for CNM-18, 0.58 for CNM-26, 0.61 for CNM-40 and 0.55 for CNM-96, larger than that of CNM-128 (0.46) or CNM-227 (0.42). Accordingly, CS-CNTs from CNM-18, CNM-26, CNM-40 and CNM-96 had relatively lower defects inside the graphite sheets than CFs from CNM-128 and CNM-227.

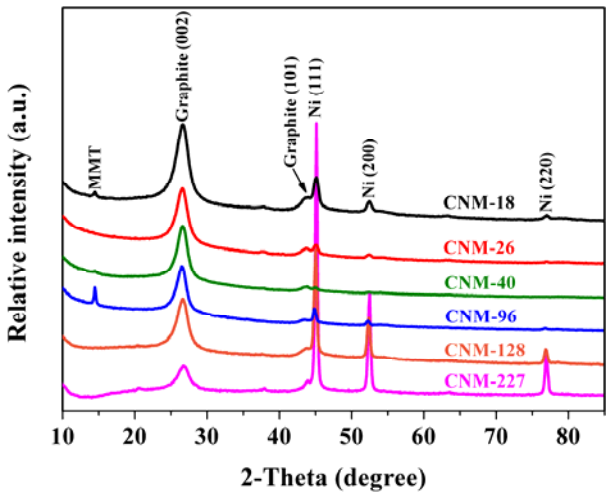

Fig. 10 XRD patterns of CNMs from PP/OMMT-NiO-x.

TGA was used to measure thermal stability of CNMs, which gave an overall quality of CNMs. Higher oxidation temperature is always associated with purer, less defective CNMs. Fig. 12 shows the derivative TGA (DTG) curves of the corresponding CNMs under air flow at a heating rate of 10 °C/min. The weight losses from 400 to 500 °C and from 500 to 650 °C were ascribed to the oxidation of amorphous carbon and CS-CNTs or CFs,[40] respectively. CNM-18, CNM-26, CNM-40 and CNM-96 showed the maximum oxidation temperature at 587.4, 587.5, 593.0 and 574.5 °C, respectively, higher than CNM-128 (560.9 °C) or CNM-227 (500.4 °C), revealing the formation of well graphitized CNMs, and/or less amorphous carbon when NiO catalysts with smaller diameter were used, consistent with the results of FE-SEM, TEM, XRD and Raman. The above results implyed that NiO catalysts with smaller diameter facilitated the formation of well graphitized CNMs, and/or prevented the formation of amorphous carbon during the carbonization of PP.

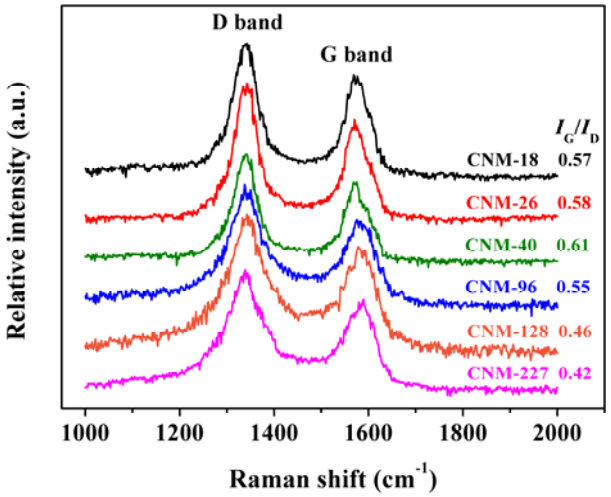

Fig. 11 Raman spectra of CNMs from PP/OMMT-NiO-x.

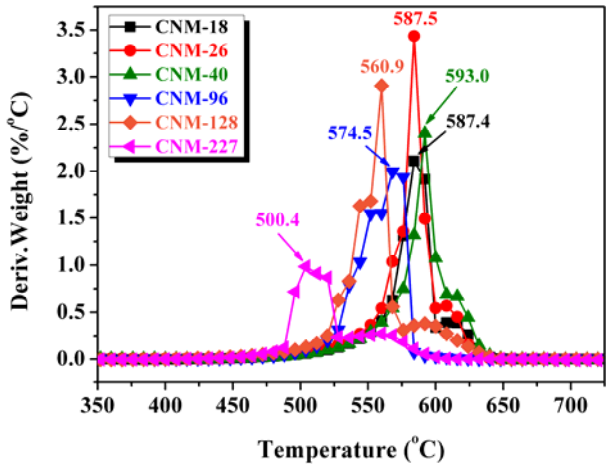

Fig. 12 DTG curves of CNMs from PP/OMMT-NiO-x under air flow at a heating rate of 10 °C/min.

3.5 Effects of NiO catalyst diameter on the coalescence and reconstruction of NiO particles

Prior to the growth of CNMs, the catalyst particles always undergo coalescence and reconstruction, and adopt well-defined geometric shapes.[41] In our previous report,[12] it was demonstrated that the coalescence and reconstruction of NiO catalysts during the carbonization of PP were crucial to the formation of CS-CNTs. To clarify the effect of NiO diameter on the coalescence and reconstruction NiO catalysts during the growth of CS-CNTs and CFs, the morphology of metallic nickel catalysts in the CS-CNTs from CNM-40, and CFs from CNM-128 and CNM-227 were observed by TEM. All of metallic nickel catalysts were located in the middle of CS-CNTs or CFs, but their shapes were different. Most of the metallic nickel catalysts in the long, straight and smooth-surface CS-CNTs showed rhombic shape with sharp

tips, while metallic nickel catalysts in the short, large and winding CFs were pear shape. However, metallic nickel catalysts in the short and large V-type CFs were irregular sphere shape.

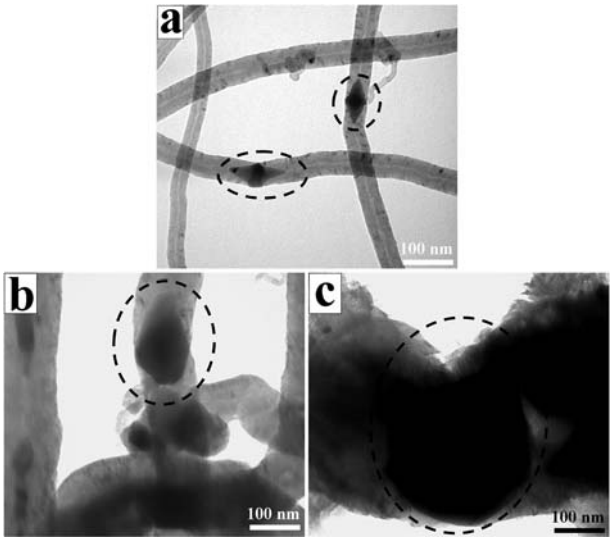

Fig. 13 Typical TEM images of metallic nickel catalysts in the CS-CNTs from CNM-40 (a), CFs from CNM-128 (b) and V-type CFs from CNM-227 (c).

Fig. 13 presents the TEM micrographs of the typical rhombic-shape Ni catalyst in CS-CNTs from CNM-40, typical pear-shape Ni catalyst in CFs from CNM-128, typical irregular sphere-shape Ni catalyst in V-type CFs from CNM-227. The diameter of rhombic-shape Ni catalysts in CS-CNTs was in the range of 40−60 nm (Fig. 13a), approximatively to the diameter of CS-CNTs from CNM-40 (57 ± 9 nm), but much larger than that of NiO-600 (14−26 nm). This is obviously ascribed to the coalescence and reconstruction of NiO catalyst nanoparticles during the carbonization of PP. Comparatively, the pear-shape Ni catalysts had a diameter range of 100−150 nm (Fig. 13b), close to the diameter of NiO-800 (128 ± 25 nm). Strikingly, for V-type CFs, the diameter of irregular sphere-shape Ni catalysts was in the range of 200−300 nm (Fig. 13c), near to the diameter of NiO-900 (227 ± 40 nm). Consequently, the coalescence and reconstruction of NiO particles during the growth of CS-CNTs, CFs and V-type CFs were different. Since the carbon sources (*i.e.*, the degradation products of PP under the catalysis of OMMT) were actually the same, it was demonstrated that NiO catalysts with smaller diameter were easily to go on coalescence and reconstruction to form rhombic shape. When the diameter of NiO catalyst increased, the reconstruction became difficult; as a result, pear-shape or irregular sphere-shape NiO catalysts were formed, which had a relatively large diameter. Hence, the diameter of CNMs increased when the diameter of NiO catalyst increased (Fig. 9b). Besides, it is well known that smaller NiO catalysts have larger surface/volume ratio, thus the number of active metal sites available for CNT nucleation increases, which favors to the formation of long CNTs and improves the yield of CNTs. This was why the yield of CNMs from PP/OMMT-NiO-x decreased with the increasing diameter of NiO catalyst (Fig. 4).

3.6 Adsorption of oils using CNMs

To explore the potential application of the resultant CNMs in the removal of oils, CNMs were used as adsorbents, and diesel, vegetable oil, kerosene and mineral oil were selected as model oils. The results are displayed in Figure 14a.

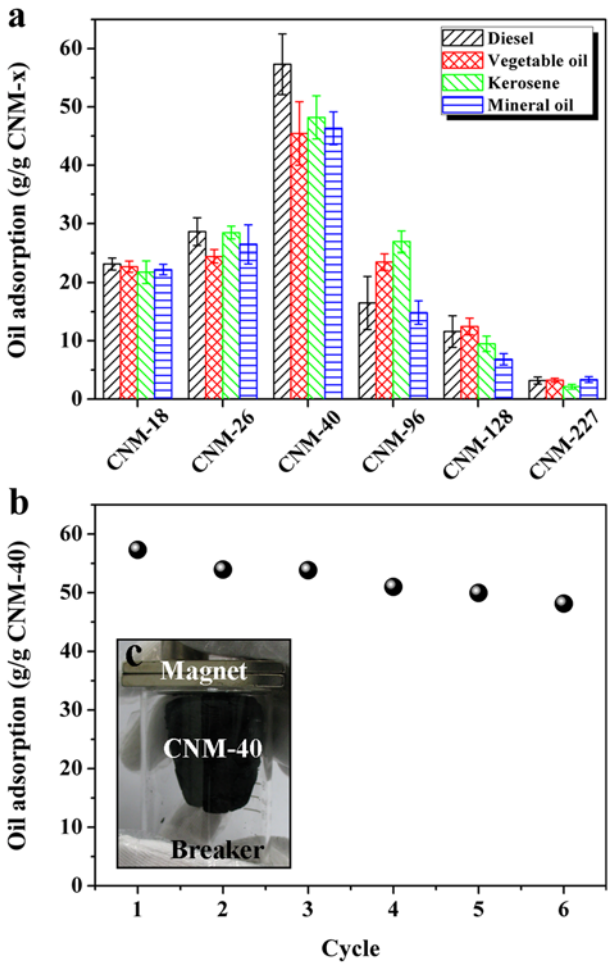

Fig. 14 Absorption of oils (diesel, vegetable oil, kerosene and mineral oil) by CNMs (a), recycling performance of diesel adsorption by sponge-like CNM-40 (b), and a picture of CNM-40 attracted by a magnet (c).

It was observed that the adsorption capacities of sponge-like CNM-40 for diesel, vegetable oil, kerosene and mineral oil were 57.3, 45.5, 48.2 and 46.3 (g/g CNM-40), respectively, much higher than those of other CNMs, while CNM-227 had lowest oils capacities. Obviously, the oil adsorption capacity of CNMs depends not only on the surface area of CNMs, but also the pore structure.[27,28] It is suggested that the high adsorption capacity for sponge-like CNM-40 comes from high BET surface area (162.6 m^2/g for CNM-40 *vs.* 118.2 m^2/g for CNM-18 or 125.9 m^2/g for CNM-227) and the intertube spaces with large-sized macropores (2–100 nm, Fig. S4). Fig. 14b shows the recycling performance of diesel adsorption by sponge-like CNM-40. After six cycles, the adsorption capacity of sponge-like CNM-40 for diesel decreased to 48.1 (g/g CNM-40). The decreased adsorption capacity was probably ascribed to the agglomeration of CS-CNTs during the calcination of CNM-40 in a muffle at 400 °C to remove the

adsorbed diesel, resulting in the destruction of some mesopores and macropores in CNM-40 as shown in the Fig. S5. Nevertheless, the sponge-like CNM-40 had a good recycling performance. Overall, compared to other adsorbents (Table 1), including activated carbon,[27] nano-wire,[42] kapok,[28] polyester sponge,[27] polyurethane sponge,[27] exfoliated graphite,[43] EV/CNT-fluffy[44] and CNT sponge,[27] sponge-like CNM-40 showed not only high capacities, good recycling performance and good mechanical property (Fig. 5c), but also magnetic separation (Fig. 14c) with wide and cheap source and simple preparation.

Table 1 Comparison of diesel adsorption capability of different adsorbent materials.

Sample	Diesel oil absorption (g/g)	Reference
Activated carbon	0.6	27
Nano-wire	20	42
Kapok	20.8–36.7	28
Polyester sponge	26	27
Polyurethane sponge	45	27
Exfoliated graphite	53	43
Sponge-like CNM-40	57.3	This work
EV/CNT-fluffy	70.6	44
CNT sponge	146	27

Conclusions

A one-pot approach was demonstrated to efficiently synthesize high value-added CNMs including sponge-like CS-CNTs and CFs through the carbonization of PP under the combined catalysts of OMMT and NiO at 700 ^{o}C. When the diameter of NiO catalyst increased from 18 to 227 nm, the yield of CNMs almost linearly decreased from 51.9 to 10.8 wt %. Meanwhile, NiO catalysts with small diameter (*e.g.*, 40 nm) promoted the formation of long, straight and surface-smooth CS-CNTs with the graphene nanosheets oblique to the CS-CNTs axis at the angle of 20−23^{o}. However, NiO catalysts with large diameter (*e.g.*, 227 nm) favored the formation of short and surface-rugged CFs. This was because NiO catalysts with small diameter were more susceptible to go on the coalescence and reconstruction into rhombic shape. When the diameter of NiO catalysts increased, the reconstruction of NiO particles became difficult. Finally, the obtained sponge-like CNM-40 showed high performance in the adsorptions of diesel, vegetable oil, kerosene and mineral oil with good recycling performance, good mechanical property and magnetic separation. It is believed that this work will help to better understand the carbonization mechanism of plastics and contribute to the conversion of waste plastics into high value-added CNMs. The applications of CS-CNTs in the energy, eviroment and catalysis fields are on the way in our laboratory.

Acknowledgements

This work was supported by the National Natural Science Foundation of China (51373171, 2124079, 51233005 and 21374114) and Polish Foundation (No. 2011/03/D/ST5/06119).

Notes and references

[a] *State Key Laboratory of Polymer Physics and Chemistry, Changchun Institute of Applied Chemistry, Chinese Academy of Sciences, Changchun 130022, China. Fax: +86 (0) 431 85262827; Tel: +86 (0) 431 85262004; E-mail: ttang@ciac.ac.cn; liujie@ciac.ac.cn*
[b] *University of Chinese Academy of Sciences, Beijing 100049, China*
[c] *Institute of Chemical and Environment Engineering, West Pomeranian University of Technology, Szczecinul. Pulaskiego 10, 70-322 Szczecin, Poland*

† Electronic Supplementary Information (ESI) available: The diameter distribution of NiO catalyst calcined at different temperature, the length distribution of CNMs, the diameter distribution of CNMs, pore size distributions of CNMs and pore size distributions of CNM-40 before and after the sixth cycle. See DOI: 10.1039/b000000x/

References

1 C. W. Zhuo and Y. A. Levendis, *J. Appl. Polym. Sci.*, 2014, **131**, 39931.
2 A. Bazargan and G. McKay, *Chem. Eng. J.*, 2012, **195–196**, 377.
3 C. F. Wu, M. A. Nahil, N. Miskolczi, J. Huang and P. T. Williams, *Environ. Sci. Technol.*, 2014, **48**, 819.
4 C. F. Wu, Z. C. Wang, L. Z. Wang, P. T. Williams and J. Huang, *RSC Adv.*, 2012, **2**, 4045.
5 J. C. Acomb, C. F. Wu and P. T. Williams, *Appl. Catal. B: Environ.*, 2014, **147**, 571.
6 C. W. Zhuo, B. Hall, H. Richter and Y. Levendis, *Carbon*, 2010, **48**, 4024.
7 C. W. Zhuo, J. O. Alves, J. A. S. Tenorio and Y. A. Levendis, *Ind. Eng. Chem. Res.*, 2012, **51**, 2922.
8 V. G. Pol and M. M. Thackeray, *Energy Environ. Sci.*, 2011, **4**, 1904.
9 T. Tang, X. C. Chen, X. Y. Meng, H. Chen and Y. P. Ding, *Angew. Chem. Int. Ed.*, 2005, **44**, 1517.
10 Z. W. Jiang, R. J. Song, W. G. Bi, J. Lu and T. Tang, *Carbon*, 2007, **45**, 449.
11 R. J. Song, Z. W. Jiang, W. G. Bi, W. X. Cheng, J. Lu, B. T. Huang and T. Tang, *Chem. Eur. J.*, 2007, **13**, 3234.
12 J. Gong, J. Liu, Z. W. Jiang, X. Wen, X. C. Chen, E. Mijowska, Y. H. Wang and T. Tang, *Chem. Eng. J.*, 2013, **225**, 798.
13 J. Gong, J. D. Feng, J. Liu, R. Muhammad, X. C. Chen, Z. W. Jiang, E. Mijowska, X. Wen and T. Tang, *Ind. Eng. Chem. Res.*, 2013, **52**, 15578.
14 J. Gong, J. Liu, L. Ma, X. Wen, X. C. Chen, D. Wan, H. O. Yu, Z. W. Jiang, E. Borowiak-Palen and T. Tang, *Appl. Catal. B: Environ.*, 2012, **117–118**, 185.
15 J. Gong, K. Yao, J. Liu, X. Wen, X. C. Chen, Z. W. Jiang, E. Mijowska and T. Tang, *Chem. Eng. J.*, 2013, **215–216**, 339.
16 J. Gong, J. Liu, Z. W. Jiang, J. D. Feng, X. C. Chen, L. Wang, E. Mijowska, X. Wen and T. Tang, *Appl. Catal. B: Environ.*, 2014, **147**, 592.
17 J. Gong, J. D. Feng, J. Liu, Z. W. Jiang, X. C. Chen, E. Mijowska, X. Wen and T. Tang, *Chem. Eng. J.*, 2014, **48**, 27.
18 J. Gong, J. Liu, D. Wan, X. C. Chen, X. Wen, E. Mijowska, Z. W. Jiang, Y. H. Wang and T. Tang, *Appl. Catal. A: Gen.*, 2012, **449**, 112.
19 J. Gong, J. Liu, X. C. Chen, X. Wen, Z. W. Jiang, E. Mijowska, Y. H. Wang and T. Tang, *Micropor. Mesopor. Mat.*, 2013, **176**, 31.
20 J. Gong, J. Liu, Z. W. Jiang, X. C. Chen, X. Wen, E. Mijowska and T. Tang, *Appl. Catal. B: Environ.*, 2014, **152–153**, 289.
21 S. S. Lee, C. G. Zhang, Z. A. Lewicka, M. J. Cho, J. T. Mayo, W. W. Yu, R. H. Hauge and V. L. Colvin, *J. Phys. Chem. C*, 2012, **116**, 10287.
22 A. Baliyan, Y. Hayasaki, T. Fukuda, T. Uchida, Y. Nakajima, T. Hanajiri and T. Maekawa, *J. Phys. Chem. C*, 2013, **117**, 683.
23 C. Altavilla, M. Sarno and P. Ciambelli, *Chem. Mater.*, 2009, **21**, 4851.

24 L. Jodin, A. C. Dupuis, E. Rouviere and P. Reiss, *J. Phys. Chem. B*, 2006, **110**, 7328.

25 M. F. L. De Volder, S. H. Tawfick, R. H. Baughman and A. J. Hart, *Science*, 2013, **339**, 535.

26 B. Pan and B. Xing, *Environ. Sci. Technol.*, 2008, **42**, 9005.

27 X. C. Gui, J. Q. Wei, K. L. Wang, A. Y. Cao, H. W. Zhu, Y. Jia, Q. K. Shu and D. H. Wu, *Adv. Mater.*, 2010, **22**, 617.

28 M. A. Abdullah, A. U. Rahmah and Z. Man, *J. Hazard. Mater.*, 2010, **177**, 683.

29 M. Endo, Y. A. Kim, T. Hayashi, Y. Fukai, K. Oshida, M. Terrones, T. Yanagisawa, S. Higaki and M. S. Dresselhaus, *Appl. Phys. Lett.*, 2002, **80**, 1267.

30 Y. A. Kim, T. Hayashi, Y. Fukai, M. Endo, T. Yanagisawa and M. S. Dresselhaus, *Chem. Phys. Lett.*, 2002, **355**, 279.

31 Q. F. Liu, W. C. Ren, Z. G. Chen, L. C. Yin, F. Li, H. T. Cong and H. M. Cheng, *Carbon*, 2009, **47**, 731.

32 G. Andrade-Espinosa, E. Muñoz-Sandoval, M. Terrones, M. Endo, H. Terrones and J. R. Rangel-Mendez, *J. Chem. Technol. Biotechnol.*, 2009, **84**, 519.

33 T. Yokozeki, Y. Iwahori, S. Ishiwata and K. Enomoto, *Compos. Sci. Technol.*, 2009, **69**, 2268.

34 I. Y. Jang, H. Ogata, K. C. Park, S. H. Lee, J. S. Park, Y. C. Jung, Y. J. Kim and Y. A. Kim, M. Endo, *J. Phys. Chem. Lett.*, 2010, **1**, 2099.

35 S. Ko, Y. Takahashi, H. Fujita, T. Tatsuma, A. Sakoda and K. Komori, *RSC Adv.*, 2012, **2**, 1444.

36 K. Saito, M. Ohtani and S. Fukuzumi, *J. Am. Chem. Soc.*, 2006, **128**, 14216.

37 C. F. Wu, J. Huang, P. T. Williams, *RSC Adv.*, 2013, **3**, 19239.

38 J. O. Alves, C. W. Zhuo, Y. A. Levendis, J. A. S. Tenório, *Appl. Catal. B: Environ.*, 2011, **106**, 433.

39 Y. Gao, G. -Y. Zong, H. -W. Bai and Q. Fu, *Chinese J. Polym. Sci.*, 2014, **32(2)**, 245.

40 C. F. Wu, Z. C. Wang and P. T. Williams, J. Huang, *Sci. Rep.*, 2013, **3**, 2742.

41 N. M. Rodriguez, A. Chambers and R. T. K. Baker, *Langmuir*, 1995, **11**, 3862.

42 J. K. Yuan, X. G. Liu, O. Akbulut, J. Q. Hu, S. L. Suib, J. Kong and F. Stellacci, *Nat. Nanotechnol.*, 2008, **3**, 332.

43 L. M. Bai and B. Y. Liu, *J. Harb. Univ. Sci. Tech.*, 2009, **14**, 81.

44 M. Q. Zhao, J. Q. Huang, Q. Zhang, W. L. Luo and F. Wei, *Appl. Clay Sci.*, 2011, **53**, 1.

Table of Contents (TOC)

Striking influence of NiO catalyst diameter on the carbonization of polypropylene into carbon nanomaterials and their high performance in the adsorption of oils

Jiang Gong, Jie Liu*, Xuecheng Chen, Zhiwei Jiang, Xin Wen, Ewa Mijowska, Tao Tang*

NiO diameter strongly influences the carbonization of PP into sponge-like CS-CNTs, showing high adsorption efficiency of oils with good recyclablity.